

RESEARCH ARTICLE

Open Access

# Rib fracture after stereotactic radiotherapy for primary lung cancer: prevalence, degree of clinical symptoms, and risk factors

Atsushi Nambu<sup>1,2\*</sup>, Hiroshi Onishi<sup>1</sup>, Shinichi Aoki<sup>1</sup>, Licht Tominaga<sup>1</sup>, Kengo Kuriyama<sup>1</sup>, Masayuki Araya<sup>1</sup>, Ryoh Saito<sup>1</sup>, Yoshiyasu Maehata<sup>1</sup>, Takafumi Komiyama<sup>3</sup>, Kan Marino<sup>4</sup>, Tsuyota Koshiishi<sup>1</sup>, Eiichi Sawada<sup>1</sup> and Tsutomu Araki<sup>1</sup>

## Abstract

**Background:** As stereotactic body radiotherapy (SBRT) is a highly dose-dense radiotherapy, adverse events of neighboring normal tissues are a major concern. This study thus aimed to clarify the frequency and degree of clinical symptoms in patients with rib fractures after SBRT for primary lung cancer and to reveal risk factors for rib fracture. Appropriate  $\alpha/\beta$  ratios for discriminating between fracture and non-fracture groups were also investigated.

**Methods:** Between November 2001 and April 2009, 177 patients who had undergone SBRT were evaluated for clinical symptoms and underwent follow-up thin-section computed tomography (CT). The time of rib fracture appearance was also assessed. Cox proportional hazard modeling was performed to identify risk factors for rib fracture, using independent variables of age, sex, maximum tumor diameter, radiotherapeutic method and tumor-chest wall distance. Dosimetric details were analyzed for 26 patients with and 22 randomly-sampled patients without rib fracture. Biologically effective dose (BED) was calculated with a range of  $\alpha/\beta$  ratios (1–10 Gy). Receiver operating characteristics analysis was used to define the most appropriate  $\alpha/\beta$  ratio.

**Results:** Rib fracture was found on follow-up thin-section CT in 41 patients. The frequency of chest wall pain in patients with rib fracture was 34.1% (14/41), and was classified as Grade 1 or 2. Significant risk factors for rib fracture were smaller tumor-chest wall distance and female sex. Area under the curve was maximal for BED at an  $\alpha/\beta$  ratio of 8 Gy.

**Conclusions:** Rib fracture is frequently seen on CT after SBRT for lung cancer. Small tumor-chest wall distance and female sex are risk factors for rib fracture. However, clinical symptoms are infrequent and generally mild. When using BED analysis, an  $\alpha/\beta$  ratio of 8 Gy appears most effective for discriminating between fracture and non-fracture patients.

**Keywords:** Stereotactic body radiotherapy, Lung cancer, Rib fracture, Chest wall injury

## Background

Stereotactic body radiotherapy (SBRT) has emerged as a new treatment for stage I lung cancer. Various articles have reported promising treatment effects [1-6]. SBRT has now come to be applied not only to medically inoperable patients, but also to operable patients. In the

near future, SBRT may become feasible as an alternative to surgery for stage I non-small lung carcinoma.

Posttreatment sequelae represent an important aspect of treatment that should always be taken into account when choosing treatment options. As SBRT is an extremely dose-dense therapy, very high doses are received by normal structures adjacent to the irradiated tumor. Various unpredictable adverse events may thus arise after SBRT. Several studies have reported complications related to SBRT for lung cancer, including radiation pneumonitis [7] and chest wall injuries such as rib fracture [8-10]. The reported frequencies of rib fracture after SBRT are generally higher than those associated with

\* Correspondence: nambu-a@gray.plala.or.jp

<sup>1</sup>Department of Radiology, University of Yamanashi, Chuo City, Yamanashi Prefecture, Japan

<sup>2</sup>Current institution: Department of Radiology, Teikyo University School of Medicine University Hospital, Mizonokuchi, Kawasaki City, Kanagawa Prefecture, Japan

Full list of author information is available at the end of the article

other methods of radiotherapy, such as tangential breast irradiation in breast-conserving therapy. However, the reported frequencies differ widely among investigators. We speculated that such discrepancies might be largely attributable to differences in the methods used to obtain the frequencies, with authors calculating frequencies based on symptomatic patients tending to report lower frequencies than using follow-up computed tomography (CT). That is, a substantial number of patients with rib fracture appear asymptomatic. If an adverse event often proves asymptomatic, clinicians should not overemphasize the risks.

The present study therefore aimed to clarify the frequency and degree of clinical symptoms in patients with rib fracture and related chest wall injuries found on follow-up CT after SBRT. In addition, we tried to identify the threshold biologically effective dose (BED) for rib fracture after SRT and risk factors for rib fracture.

## Methods

All study protocols including chart review were approved by the institutional review board, and written informed consent was obtained from each patient for both SBRT and participation in this investigation of SBRT-related rib fracture. Clinical symptoms and imaging findings were investigated prospectively, while dosimetric details were reviewed retrospectively.

## Patients

Between November 2001 and April 2009, a total of 210 patients with primary non-small cell lung carcinoma underwent SBRT as the first treatment with a curative intent in our institution. Of these, 177 patients agreed to participate in this study. The remaining 33 patients did not participate because they were unable to visit our hospital as required in the schedule defined in the study protocol.

## Radiotherapeutic methods

SBRT was performed using noncoplanar dynamic arcs or multiple static ports. A total dose of 48–70 Gy at the isocenter was administered in 4–10 fractions at the minimum dose point in the planning target volume (PTV) using a 6-MV X-ray, comprising three different methods: 48 Gy/4 fractions; 60 Gy/10 fractions; and 70 Gy/10 fractions (Table 1). The border of the PTV was almost on the 80–85% isodose line of the global maximum dose in the PTV.

After adjusting the isocenter of the PTV to the planned position with a unit comprising a CT scanner and linear accelerator, irradiation was performed under patient-controlled breath-holding and gated radiation beam switching.

## Follow-up of patients

Every patient was basically asked to visit our clinic at 3 and 6 months after the completion of radiotherapy, and every 6 months thereafter. At every visit, a thorough examination was performed, consisting of inquiry focusing on pain at the chest wall near the irradiated tumor and respiratory symptoms, physical examination by an attending radiation oncologist, blood testing, and CT. Clinical symptoms considered related to chest wall injury after SBRT were graded according to the criteria for pain in Common Terminology Criteria for Adverse Events, *version*. 3. Chest radiologists interpreted the results of CT just after the examinations. If the patient complained of pain, analgesics were prescribed as appropriate.

## CT examination

Preradiotherapeutic and follow-up CT were performed using a 16 multidetector row scanner (Aquilion 16; Toshiba Medical Systems, Otawara, Japan). The parameters for CT were as follows: peak voltage, 120 kVp; tube rotation time, 0.5 second; slice collimation, 1.0 mm (identical to reconstruction slice thickness and slice interval);

**Table 1 Characteristics of the 177 primary lung cancer patients and the tumors**

	Lung cancer patients (n = 177)
Mean age (range)	77.3 ± 7.0 (55–92)
Gender (male: female)	132:45
Pathology of the tumor (Ad: SCLC: SCC:spindle cell carcinoma*: unspecified**:unknown***)	89:7:47:1:9:24
Tumor diameter (average ± standard deviation)	8–55 mm(30.0 ± 9.1)
Tumor-chest wall distance (median)	0–53 mm(6)
**Range of follow-up period (median)	6–95 months (23)
Method of radiotherapy (48 Gy/4fr:60Gr/10fr:70Gr/10fr)	95:45:37
BED <sub>10</sub> of the isocenter (median)	96–119 Gy (105.6)

Abbreviations: Ad = adenocarcinoma, SCLC = small cell lung cancer, SCC = squamous cell carcinoma, BED = biologically effective dose.

\*Suspicious of pleomorphic carcinoma, but a definitive diagnosis was not made because of needle biopsy.

\*\*"unspecified" indicates pathologically definitive non-small cell lung carcinoma, but unspecified for the subtype.

\*\*\*"unknown" indicates clinically highly suspicious for lung cancer but no pathology obtained.

and beam pitch, 0.94. Tube currents were determined by an automatic exposure control in the CT machine and the tube current showing actual range of 110–400 mA. Contrast-enhanced CT was performed in 116 patients (67.1%) after unenhanced CT.

Data were reconstructed into 5-mm sections. Thin-section CT (slice thickness, 1 mm) was also produced for the regions that included the tumor or radiation-induced opacities targeting the affected lung.

Preradiotherapeutic CT was performed within 1 month before SRT, while follow-up CT was performed at 3 and 6 months and every 6 months thereafter.

#### Methods of CT evaluation

Serial follow-up CT was evaluated regarding the presence or absence of rib fractures and chest wall edema near the irradiated tumor in addition to routine radiological assessment by either of two board-certified chest radiologists at our clinic. Rib fracture was defined as a disruption of cortical continuity with malalignment. Distance between the tumor and chest wall (tumor-chest wall distance) was also measured on preradiotherapeutic CT. The time at which each finding first appeared after the completion of SBRT was reviewed later. Presence or absence of pulmonary emphysema and maximum transverse diameter of the tumor were also assessed on pre-radiotherapeutic CT.

#### Evaluation of dosimetry

Among the 177 patients, dosimetric details were available for review in 26 patients with rib fracture and 22 patients without rib fracture (Figure 1A). Patients without fracture were randomly sampled among those with no evidence of fracture on CT for >30 months. We set this period as a cut-off point as most rib fractures after SRT in this series had occurred within 30 months after

completion of SBRT. We were unable to obtain dosimetric data for the remaining patients because of breakdown of the data during the review of dosimetry. At the point that had received the maximum dose in the chest wall consisting of parietal pleura, ribs and intercostal muscles, BED was calculated in each case using a range of  $\alpha/\beta$  ratios (1–10 Gy), to clarify which  $\alpha/\beta$  ratio was most effective for evaluating the risk of rib fracture.

#### Data analysis

First, we calculated the incidence of rib fracture after SBRT on follow-up CT in the given follow-up periods of the patients. Incidence of rib fracture was also assessed in relation to tumor-chest wall distance, and the time of rib fracture appearance was evaluated. Incidence of rib fracture was also estimated by using a Kaplan-Meier method.

Second, we calculated the frequency of clinical symptoms in patients with and without rib fractures.

Third, Cox proportional hazard model was used to identify risk factors associated with rib fracture after SBRT. The independent variables tested comprised age, sex, maximum tumor diameter, radiotherapeutic method, and tumor-chest wall distance, for which the proportionalities of hazards had been confirmed using a Kaplan-Meier method. As there were three radiotherapeutic methods, we used two dummy variables to represent them.

Fourth, receiver operating characteristic (ROC) analysis was undertaken for maximum BED of the chest wall at each  $\alpha/\beta$  ratio. For BED at the  $\alpha/\beta$  ratio that provided the largest area under the curve, we calculated the cut-off dose that most effectively differentiated between fracture and non-fracture patients. This was regarded as the dose at the point closest in rectilinear distance on the ROC curve to point 1.0 on the vertical axis, where both sensitivity and specificity become 1.0.

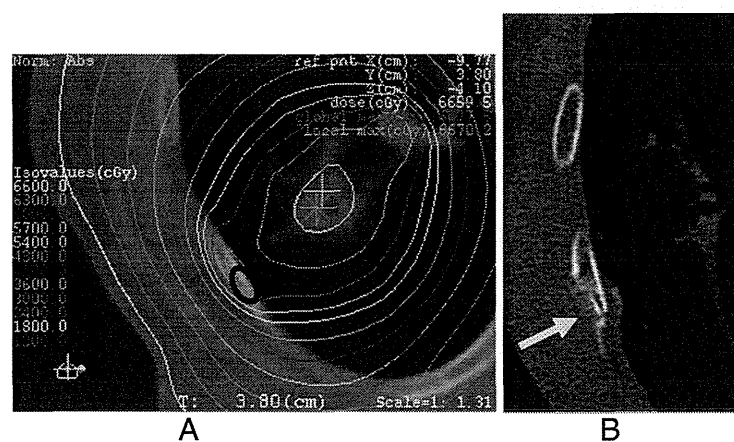


**Figure 1** An 86-year-old woman with adenocarcinoma after SRT. **A)** Dosimetry overlaying CT with a bone window shows the maximum prescribed dose to the chest wall as 63 Gy, with a  $BED_3$  of 233.2 Gy. The site of rib fracture later is indicated by a black elliptical circle. **B)** Rib fracture was noted at 24 months after completion of SRT. Amorphous osteosclerosis is also seen (arrow).

**Table 2 Appearance times and frequencies of the rib fractures and chest wall edema**

	Appearance time ranges	Frequency in fracture group (n = 41)	Frequency in non-fracture group (n = 136)
Rib fractures	4–58	41 (100)*	0 (0)
Chest wall edema	2–57	35 (85.4)	10 (7.4)

\*The numbers in the parentheses in the frequencies of findings are percentages.

Fifth, we evaluated the correlation between the timing of rib fracture appearance and BED at the  $\alpha/\beta$  ratio defined above in the 26 patients with rib fracture using Pearson's correlation coefficient.

Values of  $p < 0.05$  were considered significant in all analyses. All statistical analyses were performed using IBM SPSS Statistics version 18 software (IBM, New York, USA).

## Results

### Patient demographics

Patient demographics and tumor characteristics are summarized in Table 1. Local control rates were 91% at 1 year and 83% at 3 years (detailed data not shown).

### Incidence of rib fractures after SRT

Incidence of rib fracture was 23.2% (41/177) at a median follow-up period of 33 months (range, 24–94 months) (Figure 1). When the tumor-chest wall distance was  $\leq 25$  mm, the incidence was 27.8% (41/148). The frequency of rib fracture rose to 31.3% for a distance of  $\leq 16$  mm (41/131). No patients with a distance  $> 16$  mm developed a rib fracture. When the distance was 0, the frequency of rib fracture was 36.7% (22/60). Kaplan-Meier method estimated the incidence to be 27.4% at 24 months.

### Time-to-event for rib fracture and chest wall edema

Durations to rib fracture and other related findings are summarized in Table 2. Three patients showed rib frac-

tures  $\geq 30$  months after completion of SBRT, at 37, 53 and 58 months.

Chest wall edema was seen in 45 of 177 patients (25.4%), arising at a mean of 12 months (range, 2–57 months) (Figure 2), and appearing as asymmetrical swelling of the ipsilateral chest wall with low attenuation areas compared to the contralateral side.

### Symptoms of rib fracture

Clinical symptoms in patients with rib fracture and without rib fracture are summarized in Table 3. No patients complained of Grade 3 or more symptoms. Four patients without rib fractures complained of Grade 1 chest wall pain with all 4 cases showing radiological evidence of chest wall edema. In the study population as a whole, the frequency of chest wall pain was 21.5% (38/177). Among patients with peripheral tumors that had a tumor-chest wall distance  $\leq 25$  mm, the frequency of chest pain was 25.7%.

### Risk factors of rib fracture after SBRT

The results of Cox proportional hazard modeling are summarized in Table 4. Tumor-chest wall distance and sex were significant risk factors for rib fracture.

Area under the curve ranged from 0.781 to 0.865 and was largest for an  $\alpha/\beta$  ratio of 8 Gy ( $BED_8$ ). A  $BED_8$  value of 115.0 Gy was the most discriminative value between fracture and non-fracture patients, yielding 73% sensitivity and 91% specificity. The lowest  $BED_8$  that resulted in rib fracture was 91.1 Gy.  $BED_8$  did not

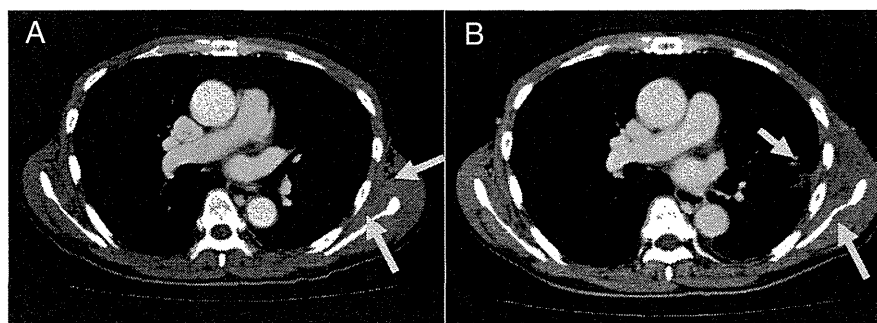


**Figure 2** A 64-year-old man with adenocarcinoma after SRT. **A)** At 3 months after completion of SRT, contrast-enhanced CT shows suspicious findings in the left chest wall, such as slight asymmetry and indistinct intermuscular fat planes (arrows). **B)** At 15 months after SRT, contrast-enhanced CT shows definitive chest wall edema, evidenced by swelling of the left chest wall with an area of low attenuation (arrows). No rib fracture was seen at this time.

**Table 3 Frequency and degree of chest wall pain**

Degree of pain*	Fracture group (n = 41)	Non-fracture group (n = 136)
Grade 0	27 (65.9)**	132 (97)
Grade 1	7 (17.1)	4 (3)
Grade 2	7 (17.1)	0 (0)
Grade 3 and 4	0 (0)	0 (0)

\*The degree of chest wall pain was evaluated according to Common Terminology Criteria for Adverse Events, Ver. 3.

\*\*The numbers in the parentheses are percentages.

correlate significantly with the timing of rib fracture appearance ( $r = -0.362$ ,  $p = 0.070$ ).

### Discussion

The frequency of rib fracture was 23.2% in our series. In Kaplan-Meier method, it was estimated to be 27.4% at 24 months after the SBRT. Reported frequencies of rib fracture after SBRT differ markedly among investigations, ranging from 3% to 21.2% [8-10]. Our result is closest to that described by Petterson et al., who reported the highest frequency of 21.2% by examining the results of follow-up CT [9]. We speculate that these discrepancies between studies are mainly attributable to differences in the methods of estimating frequency. Both Petterson, et al. and the present study obtained the frequency using follow-up CT, whereas other investigations have determined frequencies by confirming the presence of rib fracture on chest radiographs in patients complaining of chest pain. That is, asymptomatic patients with rib fracture may largely account for these discrepancies. In fact, only 34.1% of patients with rib fractures displayed clinical symptoms in our series. Differences in follow-up period, method of SRT and proportion of tumors close to chest wall may have also contributed to the discrepancies.

The frequency of chest wall pain was 21.5% (38/177) in our series. When confined to patients with a tumor-chest wall distance  $\leq 25$  mm, the frequency was 25.7%. Dunlap et al. observed that 17 of 60 patients (28%) with a peripheral tumor  $< 2.5$  cm from the chest wall had Grade 3 pain and another 3 patients (5%) had Grade 1 or 2 pain in the median follow-up period of 11.1 months. Frequency of chest wall pain in total was 33% in that series, higher than

the present study (25.7%) despite the fact that the median follow-up period in that study was much shorter than that in the present study. Furthermore, Grade 3 pain was present in a higher proportion of the subjects in their study, compared to our investigation. We speculate that this difference is mainly due to differences in radiotherapy. BEDs at the isocenter seem much higher with the method applied by Dunlap et al.

Rib fracture is considered a common adverse event on CT after SBRT for lung cancer. However, the frequency of chest wall pain in patients with rib fracture was only 34.2%. Furthermore, pain was generally mild and usually controllable using non-opioid analgesics in our series. Reducing a prescribed dose to avoid rib fracture to such a degree the tumor may be unsatisfactorily irradiated is not justified, but using more fractions with reduced dose might help to avoid adverse events. Also, it should also be noted that the frequency and degree of chest wall pain are greatly dependent on the total dose or fractions. Our BED<sub>10</sub> at the isocenter ranged from 96 to 119 Gy, which may be one of the safe ranges in terms of avoiding adverse events.

Little is known about the mechanisms by which pain is induced in chest wall injury. As most symptomatic patients had rib fracture in our series, fracture pain would be a plausible contributing factor. An animal study suggested that activation of nociceptors by mechanical stimulation or an influx of hematological and inflammatory cells into the fracture site is responsible for the pain related to fracture [11]. In contrast to rib fractures caused by trauma, those after SBRT are considered to involve a relatively chronic process and usually do not involve external force.

**Table 4 Results of Cox proportional hazard model analysis**

Independent valuable	P value	Hazard ratio	95% confidence interval
Tumor-chest wall distance (mm)	$< 0.0001$	0.858	0.801-0.920
Age	0.713	0.990	0.937-1.045
Gender*	0.002	3.172	1.503-6.695
Maximum diameter of the tumor	0.754	0.994	0.955-1.034
Radiotherapeutic method 48 Gy or not	0.829	0.911	0.391-2.122
Radiotherapeutic method 60 Gy or not	0.087	0.454	0.184-1.121

\*The hazard ratio for gender is represented as the hazard of women divided by that of men.

Nociceptors might thus be less likely to be mechanically irritated, particularly in non-weight-bearing bones like ribs. In addition, radiation-induced microcapillary injury may hamper recruitment of inflammatory cells at the site of fracture in the chronic stage, which in turn may also result in less pain.

Four patients without rib fracture complained of Grade 1 pain. These patients showed evidence of chest wall edema on follow-up CT. Chest wall inflammation or contraction of the tissue due to fibrosis, which could irritate nerves, could be another factor contributing to chest wall pain.

Cox proportional hazard analysis showed that smaller tumor-chest wall distance and female sex were independent risk factors for rib fracture after SBRT while age, maximum diameter of the tumor and, radiotherapeutic method were not statistically significant risk factors. When tumor-chest wall distance decreased by 1 mm, risk of rib fracture increased by a factor of 1.153. This result is unsurprising, given that as the distance decreases, the chest wall becomes more likely to receive a high dose of radiation. In terms of sex differences, postmenopausal women are well-known to have a higher risk of osteoporosis due to decreased bone mineralization compared with men. As women in our study population were  $\geq 55$  years old, this effect most likely explains the higher likelihood of fracture in women.

ROC analysis suggested that when using BED analysis, an  $\alpha/\beta$  ratio of 8 Gy was most effective for discriminating between fracture and non-fracture patients. The  $\alpha/\beta$  ratios for late bone damage were estimated to be within the range of 1.8–2.8 Gy, similar to those reported for other late-responding normal tissues [12]. Our results appear to contradict those of previous reports. However, it remains unclear whether the linear-quadratic model is adaptable to hypofractionated high-dose radiotherapy, such as SBRT to the lung. In addition, we used thin-section CT, which is deemed as the most sensitive and specific examination for evaluating rib fracture. This may also partly account for the discrepancy. Our results might suggest that another model is required to estimate risks of rib fracture in SBRT.

No patients with  $BED_8 < 91.1$  Gy developed rib fracture. Although 91.1 Gy as a maximum  $BED_8$  for the chest wall might suggest threshold values for rib fracture, validation studies with a larger number of patients are required.

$BED_8$  did not correlate significantly with the timing of rib fracture appearance. However, we still cannot conclude that radiation dose is unrelated to the timing of rib fracture appearance, as the number of patients evaluated was too small to reach a definitive conclusion.

Several limitations to the present study must be considered. First, for  $BED_3$  of the chest wall, not all cases from the study population were sampled. However, we believe

that our random sampling method provided a clear and concise reference value, which would offer a benchmark when considering risk of rib fracture in clinical practice. Second, although we defined the non-fracture group as cases free from rib fracture for  $>30$  months after SBRT, a few cases developed rib fractures after 30 months. In addition, there is still a possibility of second peak in the timing of rib fracture occurrence beyond our follow-up periods. Additional cases in the non-fracture group might develop rib fractures in the future and thus should be included in the fracture group. This issue may have affected our results. Third, we estimated the time at which rib fractures and other related findings appeared as that time at which these findings were first seen on follow-up CT. However, these events would actually have occurred within the intervals from the previous follow-up CT. The present study should thus be considered to have overestimated the durations to such events. Fourth, exclusion of the 33 patients who did not participate in this study may have affected our results. However, we think that this is relatively unlikely, given that the reason for nonparticipation was that these patients were unable to visit our hospital periodically, which was considered unrelated to the frequency of adverse events.

Finally, methods of SBRT for lung cancer have yet to be standardized. In fact, our radiotherapy methods varied considerably during the period of this study. Our results therefore cannot simply be applied to patients in other institutions.

## Conclusions

Rib fracture is seen with high frequency on follow-up CT after SBRT to lung cancer. Risk factors for rib fracture after SBRT include short tumor-chest wall distance, female sex and presence of pulmonary emphysema. Clinical symptoms are infrequent and mild. When using BED analysis, an  $\alpha/\beta$  ratio of 8 Gy was most effective for discriminating between fracture and non-fracture patients. However, our study was a pilot study, and thus a larger study will be required to make definitive conclusions.

## Competing interests

We have no competing interests in conducting this study and writing this paper.

## Authors' contributions

AN did image interpretation and statistical analyses and drafted the manuscript. HO gathered the clinical data, supervised this study and edited this paper. SA gathered the clinical data and recalculated the dosimetry data. LT gathered the clinical data and investigated the relationship between radiation dose and occurrence of rib fracture. KK, MA, RS, YM, TK and KM gathered the clinical data. TK investigated the relationship between the clinical symptoms and rib fractures. ES interpreted the CT images. TA supervised this study.

## Author details

<sup>1</sup>Department of Radiology, University of Yamanashi, Chuo City, Yamanashi Prefecture, Japan. <sup>2</sup>Current institution: Department of Radiology, Teikyo University School of Medicine University Hospital, Mizonokuchi, Kawasaki

City, Kanagawa Prefecture, Japan. <sup>3</sup>Department of Radiology, Kofu Municipal Hospital, Kofu City, Yamanashi Prefecture, Japan. <sup>4</sup>Department of Radiology, Yamanashi Prefectural Central Hospital, Kofu City, Yamanashi Prefecture, Japan.

Received: 30 April 2012 Accepted: 4 February 2013  
Published: 7 February 2013

## References

1. Onishi H, Araki T, Shirato H, Nagata Y, Hiraoka M, Gomi K, Yamashita T, Niibe Y, Karasawa K, Hayakawa K, Takai Y, Kimura T, Hirokawa Y, Takeda A, Ouchi A, Hareyama M, Kokubo M, Hara R, Itami J, Yamada K: Stereotactic hypofractionated high-dose irradiation for stage I nonsmall cell lung carcinoma: clinical outcomes in 245 subjects in a Japanese multiinstitutional study. *Cancer* 2004, **10**:1623–1631.
2. Nagata Y, Takayama K, Matsuo Y, Norihisa Y, Mizowaki T, Sakamoto T, Sakamoto M, Mitsumori M, Shibuya K, Araki N, Yano S, Hiraoka M: Clinical outcomes of a phase I/II study of 48 Gy of stereotactic body radiotherapy in 4 fractions for primary lung cancer using a stereotactic body frame. *Int J Radiat Oncol Biol Phys* 2005, **63**:1427–1431.
3. Nyman J, Johansson KA, Hultén U: Stereotactic hypofractionated radiotherapy for stage I non-small cell lung cancer—mature results for medically inoperable patients. *Lung Cancer* 2006, **51**(1):97–103.
4. Fritz P, Kraus HJ, Blaschke T, Mühlnickel W, Strauch K, Engel-Riedel W, Chemaissani A, Stoelben E: Stereotactic, high single-dose irradiation of stage I non-small cell lung cancer (NSCLC) using four-dimensional CT scans for treatment planning. *Lung Cancer* 2008, **60**:193–199.
5. Haasbeek CJ, Lagerwaard FJ, de Jaeger K, Slotman BJ, Senan S: Outcomes of stereotactic radiotherapy for a new clinical stage I lung cancer arising postpneumonectomy. *Cancer* 2009, **115**:587–594.
6. Onishi H, Shirato H, Nagata Y, Hiraoka M, Fujino M, Gomi K, Karasawa K, Hayakawa K, Niibe Y, Takai Y, Kimura T, Takeda A, Ouchi A, Hareyama M, Kokubo M, Kozuka T, Arimoto T, Hara R, Itami J, Araki T: Stereotactic Body Radiotherapy (SBRT) for Operable Stage I Non-Small-Cell Lung Cancer: Can SBRT Be Comparable to Surgery? *Int J Radiat Oncol Biol Phys* 2010, Epub ahead of print.
7. Takeda A, Ohashi T, Kunieda E, Enomoto T, Sanuki N, Takeda T, Shigematsu N: Early graphical appearance of radiation pneumonitis correlates with the severity of radiation pneumonitis after stereotactic body radiotherapy (SBRT) in patients with lung tumors. *Int J Radiat Oncol Biol Phys* 2010, **77**:685–690.
8. Dunlap NE, Cai J, Biedermann GB, Yang W, Benedict SH, Sheng K, Scheffer TE, Kavanagh BD, Lerner JM: Chest wall volume receiving >30 Gy predicts risk of severe pain and/or rib fracture after lung stereotactic body radiotherapy. *Int J Radiat Oncol Biol Phys* 2010, **76**:796–801.
9. Petterson N, Nyman J, Johansson KA: Radiation-induced rib fractures after hypofractionated stereotactic body radiation therapy of non-small cell lung cancer: a dose- and volume-response analysis. *Radiother Oncol* 2009, **91**:360–368.
10. Voroney JP, Hope A, Dachele MR, Purdie TG, Franks KN, Pearson S, Cho JB, Sun A, Payne DG, Bissonnette JP, Beziak A, Brade AM: Chest wall pain and rib fracture after stereotactic radiotherapy for peripheral non-small cell lung cancer. *J Thorac Oncol* 2009, **4**:1035–1037.
11. Freeman KT, Koewler NJ, Jimenez-Andrade JM, *et al*: A fracture pain model in the rat: adaptation of a closed femur fracture model to study skeletal pain. *Anesthesiology* 2008, **108**:473–483.
12. Overgaard M: Spontaneous radiation-induced rib fractures in breast cancer patients treated with postmastectomy irradiation. A clinical radiobiological analysis of the influence of fraction size and dose-response relationships on late bone damage. *Acta Oncol* 1988, **27**:117–122.

doi:10.1186/1471-2407-13-68

Cite this article as: Nambu *et al*: Rib fracture after stereotactic radiotherapy for primary lung cancer: prevalence, degree of clinical symptoms, and risk factors. *BMC Cancer* 2013 **13**:68.

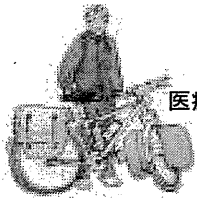
Submit your next manuscript to BioMed Central and take full advantage of:

- Convenient online submission
- Thorough peer review
- No space constraints or color figure charges
- Immediate publication on acceptance
- Inclusion in PubMed, CAS, Scopus and Google Scholar
- Research which is freely available for redistribution

Submit your manuscript at  
[www.biomedcentral.com/submit](http://www.biomedcentral.com/submit)



## 放射線治療と医学物理士



医療と技術

大谷 侑輝\*, 小泉 雅彦\*\*

Radiation therapy and Medical physicists

Key Words : Radiation therapy, Medical physics

## 1. はじめに

がんは日本人の2人に1人が罹り、死因の1位となっている重篤な国民的病気です。放射線治療は、手術や化学療法と並ぶ、がん治療の3本柱の1つとされ、その役割は多大な期待と重責を担っています。近年、放射線治療は、コンピュータの発展と共に目覚ましい技術革新を遂げ、放射線治療を受けるがん患者の割合も増加しています。

放射線治療の最大のメリットは、他の治療法に比べて身体的負担が少なく、機能や形態の温存が可能なことです。例えば、喉頭がんを手術で切除すれば発声機能が失われかねませんし、麻酔などは身体的に大きな負担となります。放射線治療ならば、発声機能を温存しつつ、良好な治療成績をあげる事が可能で、高齢者や合併症を持つ患者にも優しい治療です。

この放射線治療に携わる職種には、医師や診療放

射線技師、そして医学物理士などがあります。今回は、医学物理士にスポットを当てます。業務内容やそれを取り巻く環境、大阪大学における医学物理士育成の取り組みなどをご紹介します。

## 2. 医学物理士とは

「医学物理」という言葉に馴染みのない方も多くと思います。日本医学物理学会では、医学物理学を「理工学の知識・成果を医学に応用・活用する学術分野であり、医学・医療への貢献を通じて人類の健康に寄与する学問である」と定義しています<sup>1)</sup>。医学物理学の分野としては、放射線診断学、核医学物理学、放射線治療物理学、放射線防護・安全管理学、基礎医学物理学などがあります。これらの分野に携わる職種が医学物理士となります。最も人材が求められている分野は、放射線治療物理学です。欧米では、医学物理士数が多いため、医学物理学は学問として広く認知されています。一方で、日本では理学系や工学系の方々からの認知度が低く、医学物理士数も欧米と比べて多くありません。

欧米では、放射線治療に携わる職種として、医師、診療放射線技師、ドジメトリスト（線量計算士）、医学物理士、看護師があります。それぞれの役割が明確化されており、診療放射線技師は照射業務、ドジメトリストは治療計画補助、医学物理士は治療計画立案や品質管理業務を主に担当しています。日本では、職種による線引きが曖昧で、本来異なるはずの担当業務に重複が生じており、多くの施設では、医師が治療計画立案、診療放射線技師が品質管理業務を兼任しているのが現状です。日本の診療放射線技師は非常に優秀で学歴も高く、勤勉です。身を削って役割を担ってきました。しかし、近年の放射線治療分野における技術革新は目覚ましく、次々と高度で複雑な治療技術や装置が導入される中での兼任



\*Yuki OTANI

1981年10月生  
大阪大学大学院医学系研究科保健学専攻修了 (2011年)  
現在、大阪大学大学院医学系研究科 放射線腫瘍学講座 特任助教 保健学博士  
TEL : 06-6879-3482  
FAX : 06-6879-3489  
E-mail : y.otani@radonc.med.osaka-u.ac.jp



\*\*Masahiko KOIZUMI

1959年2月生  
京都大学大学院工学研究科博士課程修了 (1986年)  
大阪大学医学部医学科卒業 (1991年)  
現在、大阪大学大学院医学系研究科 医用物理学講座 教授 工学博士 医学博士  
TEL : 06-6879-2570  
FAX : 06-6879-2575  
E-mail : koizumi@sahs.med.osaka-u.ac.jp



業務は、過度の仕事量となり、医療事故が誘発されることは否めません。さらに、一般的に診療放射線技師は定期的な配置転換が行われるため、一定の職能を獲得しても診断部門への転向などがあります。放射線治療に専属で従事することが出来ません。もはや診療放射線技師が日々の照射業務の中で、複数業務を兼任して担えるだけの域を超えていると思われます。これらの状況を背景とし、放射線治療を専門とする職種への社会機運が高まり、医学物理士の必要性が広く認知されるまでに至りました。

### 3. 医学物理士になるためには

医学物理士は国家資格ではなく、(財)医学物理認定機構の認定資格です<sup>2)</sup>。日本における医学物理士の認定制度は1987年に開始されました。医学物理士数は2012年12月現在で673名となっています。医学物理士認定機構は、日本医学放射線学会と日本医学物理学会の代表者が設立者となり、一般財団法人として設立されました。この医学物理認定機構の課す試験に合格し、一定の要件を満たす事で医学物理士の認定を受ける事が出来ます。受験資格や認定条件の詳細は、医学物理認定機構のホームページ (<http://www.jbmp.org>) を参照して頂きたいのですが、修士以上の学位を取得して(卒業年次によって学士でも可)、医学における臨床経験を積み、認定試験に合格し、学会発表や論文などで一定以上の業績を有すれば、医学物理士になることが可能です。認定試験の合格率は約30%と若干低めですが、試験に向けた講習会なども毎年開催されており、環境は整いつつあります。

### 4. 大阪大学医学部附属病院における医学物理室の役割

大阪大学医学物理室は、2008年4月より開設されたオンコロジーセンターの放射線治療部門の下に同時に新設されました(図1)。これまでの放射線治療現場では、医師と診療放射線技師のみで治療がなされていたため、医学物理士という新職種の介入は、医師と診療放射線技師の両者から信頼を得る事から始まりました。2013年1月現在、医学物理室には、医師兼医学物理士1名と医学物理士2名の計3名が在籍しています。

医学物理室の第一の役割は、正確で安全な放射線

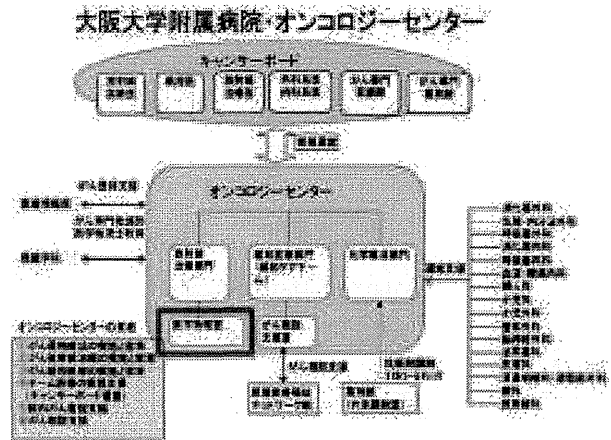


図1

治療実施のために治療計画や品質管理を行う事です。治療計画では、医師が治療標的と処方線量を決定し、医学物理士は危険臓器とビーム設定、CT撮影から治療計画の転送に至るまで全行程に関与しています。また、医学物理士は高精度放射線治療と呼ばれる強度変調放射線治療や定位放射線治療、小線源治療など複雑な治療の際は、医師と議論を交わし、治療計画の主体となります。品質管理では、各装置の性能や特徴を把握して検査する項目と頻度、調整を実施するレベルの策定をし、検査結果を解析して評価しています。

医学物理室の第二の役割は研究や教育です。研究は、新技術やソフトウェアの開発に力を入れており、治療計画検証結果や治療装置の精度を評価するソフトウェアを作成しています。新しい物理的検証方法や、Positron Emission Tomography (PET) や Magnetic Resonance Imaging (MRI) など多種画像情報の融合利用といった新治療計画システムの構築を目指し、学術研究面での国内外への情報発信を積極的に行っています。教育は、臨床実務を卒業後に短期間で実施することの出来る、即戦型医学物理士の養成に主眼を置いています。医学物理士としての臨床経験を積むため、教員の医学物理士と共に on the job training (OJT) を2年以上かけて行い、その能力を養うよう努めています。座学としては、医学部と理学部の教員が連携して提供しているため、それぞれの分野の専門的な知識を得る事が可能です。また、海外交流も積極的に行っています。日本学術振興会・先端研究拠点事業 Core-to-Core Program と

して、オランダの Groningen 大学とアメリカのインディアナ大学と教育研究交流を行っています (図 2)。現在、博士後期過程に在籍している 2 人の学生は留学中です。

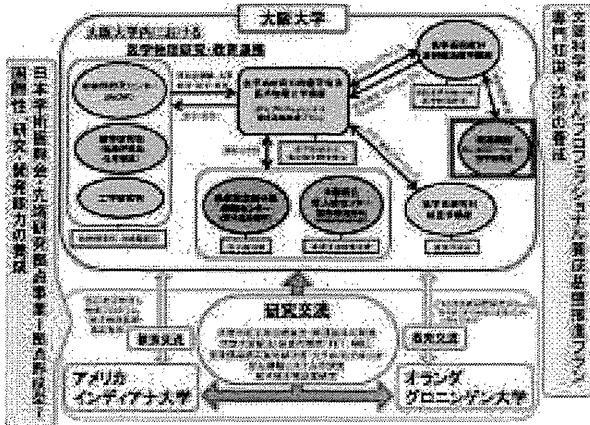


図 2

### 5. 大阪大学大学院における医学物理士養成コースのご紹介

大阪大学大学院では、2010年に医学物理士養成コースを医学科と保健学科に開設しました。医学科コースは、臨床に近い研究と医学物理士としての臨床業務の修得、保健学科コースは、医学物理の基盤と次世代粒子線治療の研究と開発を目的としています。欧米では、臨床と基礎の2コース併設が標準となっていますが、日本では大阪大学のみです(2012年12月現在)。学生は、今まで受けてきた教育の背景に応じて双方の教育環境を利用して不足部分を補強し、優位部分を伸ばすことを目指しています。両コースは人材交流も積極的に行っており、合同でカンファレンスや進捗報告会、抄読会を定期的に行っています(図3)。欧米標準に最も近い、最先端のレベルの高い教育と研究環境を提示できると考えています。

大阪大学大学院の医学物理士養成コースは、医学物理士認定機構から医学物理教育コースの施設認定を受けています(2012年度現在は暫定認定で、他大学も同様)。この認定を受けた事で、在籍する学生は1年以上在籍で医学物理士認定試験の受験資格を得る事が出来ます。また、通常は臨床経験として数える事が出来ない在学期間を、特別に臨床経験年

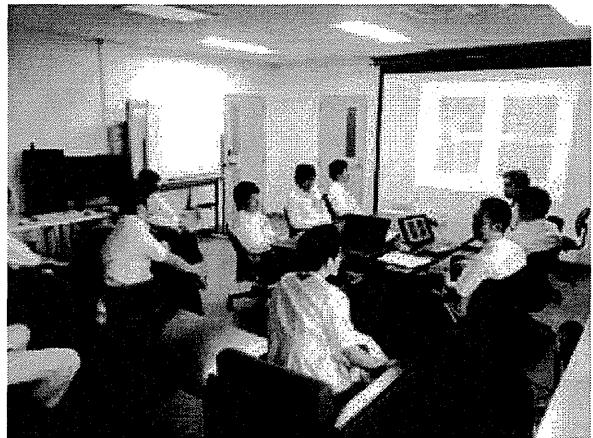


図 3

数として加算することが可能です。そのため、大阪大学大学院の医学物理士養成コースに在籍する学生は、施設認定を受けていない大学に在籍する方よりも、早く医学物理士の認定を受ける事が可能です。

### 6. 日本の医学物理士の現状

医学物理士の代表的な就職先として、研究所や放射線治療関連企業、一般病院や大学教員が挙げられます。以前は、医学物理士の社会的認知度が低いこともあって受け皿が多くありませんでしたが、ここ数年で医学物理士の需要が供給を上回るまでになりました。特に、一般病院から臨床業務が可能な医学物理士が求められています。がん患者の増加から、放射線治療装置の新規導入や増設する施設が相次ぎ、人材が不足していることに加え、平成20年度の診療報酬改定によって医療機器安全管理料2が加算されたことも大きな要因の一つです。この医療機器安全管理料2の算定要件には「放射線治療に係る医療機器の安全管理、保守点検及び安全使用のための精度管理を専ら担当する技術者が1名以上いること」と記載されています。つまり、品質管理の専門家を配置すれば診療報酬が加算されるため、病院にとってもメリットになります。現在は、大学の教員になる医学物理士も増加しています。厚生労働省の「がん対策基本法」、文部科学省の「がんプロフェッショナル養成プラン」(以下、がんプロ)の影響で、医学物理士を雇用する大学や施設が増加したためです<sup>3)</sup>。

上記では、景気の良いお話を致しましたが、数年

後も同様であるかは、分かりません。がんプロ教員は任期付のため継続雇用が不安視されると同時に、医学物理士の養成が本格的に開始されて、近い将来に供給の急激な増加が予想されるためです。医学物理士は国家資格ではないので、その人物が持っている能力が評価の対象となります。医学物理士と言えど誰でも歓迎される時期は過ぎたと思います。臨床現場から問題点を見つけ出し、自らそれを解決出来る人材が求められています。

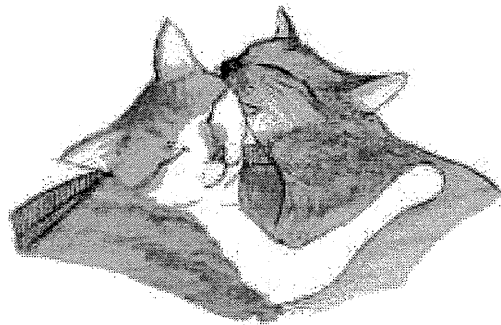
## 7. おわりに

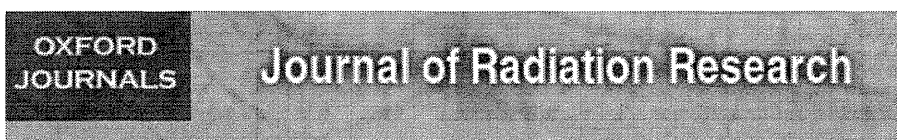
放射線治療と医学物理士の現状について、概説致しました。放射線治療や医学物理士に関してこれまで馴染みが無かった方も、この総説を読んで興味を持って頂ければ、これ以上の喜びはありません。

本原稿の執筆の機会を下さった大阪大学大学院医学系研究科・松浦成昭教授、ならびに本稿執筆にあたりお世話になった「生産と技術」各関係者の方々に厚く御礼申し上げます。

## 参考文献

- 1) 一般財団法人 日本医学物理学会  
<http://www.jsmp.org/>
- 2) 一般財団法人 医学物理士認定機構  
<http://www.jbmp.org/>
- 3) 文部科学省がんプロフェッショナル養成基盤推進プラン  
[http://www.mext.go.jp/a\\_menu/koutou/kaikaku/1314727.htm](http://www.mext.go.jp/a_menu/koutou/kaikaku/1314727.htm)





J Radiat Res. 2013 July; 54(4): 663–670.

PMCID: PMC3709659

Published online 2013 January 7. doi: [10.1093/jrr/rrs130](https://doi.org/10.1093/jrr/rrs130)

## High-dose-rate interstitial brachytherapy for gynecologic malignancies—dosimetric changes during treatment period

[Tsuayoshi Onoe](#),<sup>1,\*</sup> [Takayuki Nose](#),<sup>2</sup> [Hideomi Yamashita](#),<sup>1</sup> [Minoru Yoshioka](#),<sup>3</sup> [Takashi Toshiyasu](#),<sup>3</sup> [Takuyo Kozuka](#),<sup>3</sup> [Masahiko Oguchi](#),<sup>3</sup> and [Keiichi Nakagawa](#)<sup>1</sup>

<sup>1</sup>Department of Radiology, Tokyo University Hospital, 7-3-1 Hongo, Bunkyo-ku, Tokyo 113-8655, Japan

<sup>2</sup>Department of Radiation Oncology, Nippon Medical School Tama Nagayama Hospital, 1-7-1 Nagayama, Tama-shi, Tokyo 206-8512, Japan

<sup>3</sup>Department of Radiation Oncology, The Cancer Institute Hospital of the Japanese Foundation for Cancer Research, 3-8-31, Ariake, Koto-ku, Tokyo 135-8550, Japan

\*Corresponding author. Tel: +81-3-3815-5411; Fax: +81-3-5800-8786; E-mail: [tsuyopon13@gmail.com](mailto:tsuyopon13@gmail.com)

Received March 20, 2012; Revised December 3, 2012; Accepted December 3, 2012.

Copyright © The Author 2013. Published by Oxford University Press on behalf of The Japan Radiation Research Society and Japanese Society for Therapeutic Radiology and Oncology.

This is an Open Access article distributed under the terms of the Creative Commons Attribution Non-Commercial License

(<http://creativecommons.org/licenses/by-nc/3.0/>), which permits unrestricted non-commercial use, distribution, and reproduction in any medium, provided the original work is properly cited.

### Abstract

Go to:

To overcome cranio-caudal needle displacement in pelvic high-dose-rate interstitial brachytherapy (HDRIB), we have been utilizing a fullystretched elastic tape to thrust the template into the perineum. The purpose of the current study was to evaluate dosimetric changes during the treatment period using this thrusting method, and to explore reproducible planning methods based on the results of the dosimetric changes. Twenty-nine patients with gynecologic malignancies were treated with HDRIB at the Cancer Institute Hospital. Pre-treatment and post-treatment computed tomography (CT) scans were acquired and a virtual plan for post-treatment CT was produced by applying the dwell positions/times of the original plan. For the post-treatment plan, D90 for the clinical target volume (CTV) and D2cc for the rectum and bladder were assessed and compared with that for the original plan. Cranio-caudal needle displacement relative to CTV during treatment period was only  $0.7 \pm 1.9$  mm. The mean D90 values for the CTV in the pre- and post-treatment plans were stable (6.8 Gy vs. 6.8 Gy) and the post-treatment/pre-treatment D90 ratio was  $1.00 \pm 0.08$ . The post-/pre-treatment D2cc ratio was  $1.14 \pm 0.22$  and the mean D2cc for the rectum increased for the post-treatment plan (5.4 Gy vs. 6.1 Gy), especially when parametrial infiltration was present. The mean D2cc for the bladder was stable (6.3 Gy vs. 6.6 Gy) and the ratio was  $1.06 \pm 0.20$ . Our thrusting method achieved a stable D90 for the CTV, in contrast to previous prostate HDRIB reports displaying reductions of 35–40% for D90 during the treatment period.

**Keywords:** interstitial brachytherapy, needle displacement, gynecologic malignancy, dose–volume histogram

### INTRODUCTION

Go to:

For gynecologic tumors unsuitable for standard intracavitary brachytherapy, such as recurrent tumors or tumors with excessive invasion to the vagina/parametrium, interstitial brachytherapy has been used to achieve better tumor coverage [1–3]. Contemporary planning software for high-dose-rate interstitial brachytherapy (HDRIB) using pre-treatment computed tomography (CT) images enables a conformal dose

distribution to a target, while minimizing doses to organs at risk (OARs). To reproduce the plan in actual irradiation, relative locations of applicator needles to the clinical target volume (CTV) and OARs should also be reproduced exactly at each treatment session. However, in the literature on prostate HDRIB, needle displacements as high as 18–42 mm in the cranio-caudal direction have been reported, resulting in decreases of 35–40% in CTV coverage [4–7]. Displacements in other directions have never been explored. The needle-template unit in these studies was not sufficiently stabilized to a target. To overcome the caudal force exerted by perineal edema, we have been utilizing cranial force from fully stretched elastic tapes thrusting the template into the perineum. The purpose of the current study was to explore dosimetric changes caused by these dimensional (3D) displacements and organ mobility or deformation, to ensure safe delivery of the HDRIB treatment. To the best of our knowledge, this is the first study to report dose–volume histogram (DVH) changes during the treatment period for gynecologic HDRIB.

## MATERIAL AND METHODS

Go to:

### Patients

Between March 2006 and October 2008, 29 patients with gynecologic cancer (cervix 21, corpus 7, vulva 1) were treated at the Cancer Institute Hospital using HDRIB in combination with/without external beam radiotherapy. Patient characteristics are summarized in Table 1. Fourteen patients displayed non-recurrent disease, and 15 patients displayed recurrent disease following surgery ( $n = 12$ ), radiation ( $n = 1$ ) or both ( $n = 2$ ).

**Table 1.**  
Patient characteristics

### Methods

**Implantation and CT acquisition** Thirteen patients were treated with tandem and needles and 16 patients with needle alone. Mean number of needles used was  $18 \pm 4$  (range 9–28). All needles and the template were unified with stopper screws and the template was sutured to the perineum using six silk stitches. To overcome the caudal movement resulting from perineal edema, the needle-template unit was thrust into the perineum using two fully stretched elastic tapes of about 30 cm in length (ELASTIKON®; Johnson & Johnson, New Brunswick, NJ) attached from the ventral skin near the umbilicus through both sides of the template to the dorsal skin at the umbilical level.

About 3 h after implantation, pre-treatment CT for planning was performed. A post-treatment CT was taken prior to removal of the implant after the last treatment session. Both CT scans were performed with the bladder filled with about 200 ml saline. The interval between the two CTs was  $3.4 \pm 0.8$  days (range 2–6 days).

**Treatment planning** Planning was performed using pre-treatment CT data transferred to a planning computer (PLATO BPS® ver. 14.3.5; Nucletron, Veenendaal, the Netherlands). A central plane and the basal dose points were determined according to the extrapolated Paris system. Geometrical optimization with manual adjustments was used to achieve CTV coverage, and to keep doses for OARs below ceiling doses, and to keep hyperdose sleeves within 8–10 mm. When these three conditions (CTV coverage, OAR doses, hyperdose sleeve) could not be achieved simultaneously, the plan was clinically compromised. The selected isodose surface ( $85.4 \pm 2.4\%$  basal dose isodose surface (BDIS)) covering CTV was essentially chosen for dose prescription. The prescribed dose was 6.0 Gy per fraction to this isodose surface.

**Organ delineation** For each set of CT images, the CTV, rectum, bladder and the urethra were delineated by a single radiation oncologist (T.O.) and reviewed by another who is certified (T.N.) to eliminate inter-observer variation. The CTV, including all the areas of gross and potentially microscopic disease which consisted of the vagina, the parametrial tissues and the uterus, was delineated on each slice using clinical information,

CT/magnetic resonance imaging (MRI) and the implanted markers. For OARs, only the outer surface of the rectum, bladder and urethra were contoured and all of the volume inside the outer surface was utilized for the indices following GEC-ESTRO recommendations [8]. The rectum was delineated from the sigmoid colon curvature to the caudal level of ischial tuberosity. For the urethra, the outer surface of the Foley catheter was contoured from the bladder base to the external urethral meatus.

**Dosimetric analysis** A virtual plan for post-treatment CT was produced by duplicating the air kerma strength for the Ir-192 source, the dwell times and positions of the original plan. Dosimetric analysis was performed using the GEC-ESTRO recommendations [8]. To evaluate the coverage of the target, the dose received by 90% of the CTV (=D90) was generated. For OARs, the minimum doses to the most irradiated 2 cm<sup>3</sup> portions (=D2cc) for the rectum and bladder were generated. The dose to 50% of the urethra (=D50) was evaluated according to a study by Akimoto [9]. For each index, %BDIS and the ratio of post-treatment value to pre-treatment value was generated. All statistical analyses were performed using Dr.SPSS II (SPSS, Chicago, IL, USA). The Wilcoxon signed-rank test was used to compare DVH parameters between pre-treatment and post-treatment plans.

## RESULTS

Go to:

### Needle displacement relative to CTV centroid

Needle displacement relative to CTV centroid during treatment period was  $0.5 \pm 2.1$  mm in the lateral direction (minus (right)–plus (left)),  $1.6 \pm 3.9$  mm in the dorso-ventral direction (minus (dorsal)–plus (ventral)) and  $-0.7 \pm 1.9$  mm in the cranio-caudal direction (minus (caudal)–plus (cranial)).

### Volumetric and dosimetric results of the CTV and OARs

The volumetric and dosimetric results of CTV and OAR for the rectum, bladder and urethra are presented in Table 2. The CTV volumes showed a slight decrease during treatment ( $77.7 \pm 45.5$  cm<sup>3</sup> vs.  $73.8 \pm 41.1$  cm<sup>3</sup>), but the CTV doses were stable for both D90 values ( $6.8 \pm 0.7$  Gy vs.  $6.8 \pm 0.9$  Gy). No difference was seen in the volumes for OARs between the pre- and post-treatment plans, but dosimetric results varied among the organs. For the rectum, the mean D2cc increased from  $5.4$  Gy  $\pm$   $1.1$  Gy to  $6.1$  Gy  $\pm$   $1.5$  Gy ( $P < 0.01$ ). For the bladder, the mean D2cc tended to increase from  $6.3 \pm 1.8$  Gy to  $6.6 \pm 2.1$  Gy ( $P = 0.16$ ). The mean D50 values for the urethra in the pre- and post-treatment plans were  $3.7 \pm 1.1$  Gy vs.  $3.6 \pm 1.0$  Gy ( $P = 0.22$ ).

Table 2.

Volumetric results in CTV and OARs (rectum, bladder, urethra and sigmoid colon)

### Dosimetric analysis for the CTV and OARs

The post-/pre-treatment D90 ratio for the CTV was  $1.00 \pm 0.08$  (range 0.83–1.26). For 72.4% (=21/29) of the patients, the difference between pre- and post-treatment D90 for the CTV was within  $\pm 5\%$ . The post-/pre-treatment D90 ratio was poorly correlated with cranio-caudal needle displacement:  $0.95 \pm 0.09$  with displacement  $\geq 3.0$  mm ( $n = 4$ ) vs.  $1.01 \pm 0.07$  with displacement  $< 3.0$  mm ( $n = 25$ ). Volume changes for the CTV also had little influence on the post-/pre-treatment D90 ratios, which were  $1.01 \pm 0.08$  in cases with volume increase ( $n = 9$ ) vs.  $0.97 \pm 0.05$  in cases with volume reductions ( $n = 20$ ).

The post-/pre-treatment D2cc ratios for the rectum and bladder were  $1.14 \pm 0.22$  (range 0.71–1.63) and  $1.06 \pm 0.20$  (range 0.67–1.48), respectively. The post-/pre-treatment D2cc ratio for the rectum was significantly higher when parametrial infiltration was present ( $1.22 \pm 0.11$ ,  $n = 17$ ) than when absent ( $1.02 \pm 0.15$ ,  $n = 12$ ). The post-/pre-treatment D2cc ratio for the bladder was significantly higher when tandem use was present ( $1.13 \pm 0.17$ ) than when absent ( $1.01 \pm 0.21$ ), and also higher when cranio-caudal displacement was  $< 3.0$  mm ( $1.09 \pm 0.20$ ), compared with displacement  $> 3.0$  mm ( $0.90 \pm 0.10$ ). Lower vaginal infiltration and post-hysterectomy status showed little impact on dosimetry for the CTV and OARs (Table 3).

Table 3	Dosimetric analysis of the dose ratio of post-treatment/pre-treatment CT planning according to locations			
Mean D90	65.4 ± 3.0	58.5 ± 2.0	58.5 ± 2.0	58.5 ± 2.0
SD D90	10.2 ± 0.8	10.2 ± 0.8	10.2 ± 0.8	10.2 ± 0.8
Mean D2cc	24.1 ± 0.8	24.1 ± 0.8	24.1 ± 0.8	24.1 ± 0.8
SD D2cc	3.0 ± 0.2	3.0 ± 0.2	3.0 ± 0.2	3.0 ± 0.2
Mean D50	52.5 ± 1.5	52.5 ± 1.5	52.5 ± 1.5	52.5 ± 1.5
SD D50	15.1 ± 0.5	15.1 ± 0.5	15.1 ± 0.5	15.1 ± 0.5
Mean D90	140.1 ± 30.3	140.1 ± 30.3	140.1 ± 30.3	140.1 ± 30.3
SD D90	30.3 ± 1.0	30.3 ± 1.0	30.3 ± 1.0	30.3 ± 1.0

Table 3.

Dosimetric analysis of the dose ratio of post-treatment/pre-treatment CT planning according to locations

Figure 1 shows the frequency distributions of the post-/pre-treatment D90 ratios for the CTV and OARs. The distribution for the D90 ratio shows a narrow range with a large peak at around 1.00, whereas the distribution for D2cc ratios for the rectum and bladder displayed a relatively wide distribution. The urethra D50, however, showed a narrow range with a peak at around 1.00 similar to the distribution for the D90 ratio for the CTV.

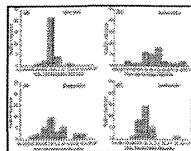


Fig. 1.

Frequency distribution chart for post-/pre-treatment ratios of CTV and OARs. (a) Abscissa: post-/pre-treatment ratios of D90 for CTV.

Ordinate: number of patients. Distribution approximates Gaussian and has steep peak, with a mean ratio of  $1.00 \pm \dots$

### Dosimetric analysis (%BDIS)

For %BDIS of mean dose at pre-treatment planning, the CTV mean was the highest ( $140.1 \pm 30.3\%$ ) followed by that of the urethra ( $52.5 \pm 15.1\%$ ), rectum ( $36.3 \pm 9.8\%$ ) and bladder ( $24.1 \pm 7.7\%$ ). The pre-treatment %BDIS of rectal D2cc was higher when parametrial infiltration was present ( $85.2 \pm 9.1\%$ ) than when absent ( $73.5 \pm 18.1\%$ ) ( $P = 0.05$ ). To assess the relationships between relative locations of CTV for each OAR and applicator, a scattergram was generated comparing the post-/pre-treatment dose ratios and %BDIS at pre-treatment planning (Fig. 2a and b). For CTV D90 and urethra D50, the ratios were distributed around 1.00 regardless of the pre-treatment %BDIS of the mean dose. The post-/pre-treatment ratios for D2cc for the rectum in cases with %BDIS of D2cc at pre-treatment planning  $\leq 90\%$  and  $>90\%$  were  $1.20 \pm 0.19$  and  $0.91 \pm 0.19$  ( $P = 0.03$ ). The corresponding ratios for bladder D2cc were  $1.10 \pm 0.21$  and  $1.03 \pm 0.18$  ( $P = 0.31$ ).

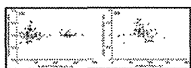


Fig. 2.

(a) Correlation between the dose ratio (ordinate: post-/pre-treatment dose ratio) and the relative locations at pre-treatment planning

(abscissa: %BDIS (6 Gy = 100%) of mean dose at pre-treatment planning) for CTV and OARs. Red = CTV mean, brown = rectum ...

### DISCUSSION

Go to:

Recent planning software for HDRIB enables conformal dose distribution to a target, while minimizing doses to OARs. According to the ICRU 58, PTV is identical to CTV since the applicators move with the CTV [10] and relative locations of brachytherapy needles should be identified at each treatment session to reproduce the plan in actual irradiation. In previous reports for prostate HDRIB, however, only cranio-caudal needle displacements have been explored and have been reported to peak as high as 18–42 mm, which caused a reduction in the D90 for the prostate of 30–40% [4–7]. In our study, cranio-caudal displacement was only  $0.7 \pm 1.9$  mm, obtained by using our fixation method with fully stretched elastic tapes. Displacements were also shown in other directions,  $0.5 \pm 2.1$  mm in the lateral and  $1.6 \pm 3.9$  mm in the dorso-ventral directions. In pelvic HDRIB, this is the first study to investigate DVH changes of CTV and OARs by these 3D displacements and also to demonstrate DVH changes during gynecologic HDRIB treatment.

In contrast to previous prostate HDRIB reports, D90 for the CTV showed no change between pre-treatment ( $6.8 \pm 0.7$  Gy) and post-treatment ( $6.8 \pm 0.9$  Gy) and the deviation of the post-/pre-treatment D90 ratio was also small ( $1.00 \pm 0.08$ ). Using our simple fixation method, cranio-caudal needle displacement relative to CTV was nearly negligible and good CTV coverage was obtained during HDRIB treatment. Lateral and dorso-ventral displacements were also small enough that D90 did not change for the CTV.

The resultant CTV coverage and small deviation of the post-/pre-treatment D90 ratio for CTV in the current



study are similar to results of our previous *in vivo* dosimetry study on pelvic HDRIB for 66 patients in which the same fixation method was used [11]. The compatibility ratio of the measured/calculated doses for the target (vaginal wall) was excellent ( $91 \pm 8\%$ ). Moreover, a 9% negative shift was considered to be attributed to the lack of inhomogeneity correction in the software for the vaginal cylinder, which has a density of 1.24. The small deviation of the compatibility ratio was largely attributable to our fixation method with fully stretched tape and synchronization in movement and deformation between the CTV and the applicator. The CTV was always deformed slightly due to the surrounding organs, but when the applicators were implanted into the target, a 'CTV–template–needle complex' was formed. The target always moved or deformed synchronously with the applicator, and applicator movement in the dorso-ventral or lateral directions had little influence on CTV coverage. Consequently, CTV coverage was not changed between pre-treatment and post-treatment CT.

We found that a large deviation was seen in post-/pre-treatment D2cc for both the rectum and bladder, which was also similar to the results of our *in vivo* dosimetry study. The rectum and bladder were independently deformed and inflated regardless of applicator movement. As a result, the distance from the applicator was varied during treatment. When the distance from the applicator was reduced, the doses increased. In this study, rectal dose increased from 5.4 Gy to 6.1 Gy and the deviation of post-/pre-treatment D2cc ratio was large ( $1.14 \pm 0.22$ ), and bladder dose tended to increase from 6.3 Gy to 6.6 Gy and the deviation was also large ( $1.06 \pm 0.20$ ). Furthermore, great variability was seen in the post-/pre-treatment volume ratios for both the rectum ( $1.18 \pm 0.68$ ) and bladder ( $1.03 \pm 0.33$ ). The patient must stay in bed during implantation because applicators protrude from the perineum, thus defecation or degassing by her own efforts is quite difficult. Similarly, a predetermined amount of injection into the bladder was sometimes difficult because of severe irritation.

There is not enough space between the rectum and the applicators, so the rectum gets covered by higher dose areas (=6.0 Gy iso-dose line) when expanded. The result of this study indicates that the rectal dose was more easily increased in patients with parametrial infiltration and/or in cases of %BDIS of D2cc for rectum  $>90\%$  at pre-treatment planning. When parametrial infiltration existed, it was necessary to implant needles in the parametrium, the lateral to the rectum. This method made the rectum expansion restricted, which results the rectal dose being easily increased (Fig. 3a and b). The %BDIS =90% region was nearly equivalent to the region of the peripheral area of the CTV. In cases of %BDIS of D2cc at pre-treatment planning  $\leq 90\%$ , the organ had inflatable space for applicators while little space was available in cases of %BDIS of D2cc  $>90\%$ . In order to avoid unexpected higher rectal doses, a degassing method should be considered when rectal inflation is observed with fluoroscopy or CT.

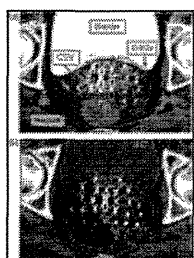


**Fig. 3.**

Transverse CT image of dose distribution of HDRIB planning at the time of (a) the pre-treatment planning and (b) the post-treatment planning.

D (reference isodose (6 Gy)) = green, CTV = red, rectum = brown, bladder = blue, urethra = purple. CTV–template–needle ...

On the other hand, the bladder has enough space to distend ventrally or cranially as well as posteriorly. Therefore, the distance from applicator changes little with changes in bladder volume. In this study, 200 ml saline was injected in each treatment session in order to fill the bladder. In gynecologic brachytherapy, the full bladder technique has been recommended to reduce the dose to the small intestine and sigmoid colon. In some reports for gynecologic intracavitary brachytherapy with CT-based 3D planning, bladder-filling control can lead to a significant reduction in the dose to the small bowel without exceeding the bladder dose [12–13].

In contrast, the post-/pre-treatment D50 ratio for the urethra was  $1.00 \pm 0.12$ , showing a similar deviation to D90 for CTV. The scattergram pattern in the urethra also displayed similar characteristics to the CTV D90. The urethra was a less deformed or inflated organ, and applicators were implanted in parallel in the dorsal and lateral spaces of the urethra, urethral movement was synchronized with the applicators and urethral



coverage was stable during HDRIB treatment.

To successfully achieve the treatment goal of HDRIB treatment for gynecological malignancies, the first consideration has to be the reproduction of the CTV and the needle-template unit position for each treatment. With our simple fixation method, cranio-caudal needle displacement is small and a highly reproducible CTV coverage is expected during HDRIB treatment. To control bladder and rectal volume at each treatment session is also important but is difficult. This requirement can be met by use of the recent image-guided methods, which are capable of providing volume images of soft-tissue organs. If large cranio-caudal displacements are confirmed, an increased margin around the CTV or a dose increment for the prescription dose is required as a safety margin. However, these increases need to be evaluated with clinical judgement because D2cc for the rectum and bladder will also rise as a result.

Finally, we used HDRIB with metal applicators in this study. However, metal applicators cause artifacts on CT images, making it difficult to draw organ contours. Some groups are performing image-based brachytherapy by using plastic/titanium applicators compatible with MRI [14–15]. We also plan to start MRI-based image-guided HDRIB.

In conclusion, with our simple method of fixing the needle-template unit using elastic tapes, needle displacement relative to the CTV was nearly negligible and excellent CTV coverage was achieved at the final treatment session. The difference between pre- and post-treatment D90 for the CTV was within  $\pm 5\%$  for 72.4% (21 of 29) of the patients in most cases.

## FUNDING

Go to:

This study was partly supported by a Grant-in-Aid for Cancer Research from the Ministry of Health, Labour and Welfare of the Government of Japan (21-8-2).

## REFERENCES

Go to:

1. Nag S, Martinez-Monge R, Selman AE, et al. Interstitial brachytherapy in the management of primary carcinoma of the cervix and vagina. *Gynecol Oncol.* 1998;70:27–32. [[PubMed](#)]
2. Martinez A, Edmundson GK, Cox RS, et al. Combination of external beam irradiation and multiple-site perineal applicator (MUPIT) for treatment of locally advanced or recurrent prostatic, anorectal, and gynecologic malignancies. *Int J Radiat Oncol Biol Phys.* 1985;11:391–8. [[PubMed](#)]
3. Monk BJ, Tewari K, Burger RA, et al. A comparison of intracavitary versus interstitial irradiation in the treatment of cervical cancer. *Gynecol Oncol.* 1997;67:241–7. [[PubMed](#)]
4. Hoskin PJ, Bownes PJ, Ostler P, et al. High dose rate afterloading brachytherapy for prostate cancer: catheter and gland movement between fractions. *Radiother Oncol.* 2003;68:285–8. [[PubMed](#)]
5. Mullokandov E, Gejerman G. Analysis of serial CT scans to assess template and catheter movement in prostate HDR brachytherapy. *Int J Radiat Oncol Biol Phys.* 2004;58:1063–71. [[PubMed](#)]
6. Damore SJ, Syed AM, Puthawala AA, et al. Needle displacement during HDR brachytherapy in the treatment of prostate cancer. *Int J Radiat Oncol Biol Phys.* 2000;46:1205–11. [[PubMed](#)]
7. Simnor T, Li S, Lowe G, et al. Justification for inter-fraction correction of catheter movement in fractionated high dose-rate brachytherapy treatment of prostate cancer. *Radiother Oncol.* 2009;93:253–8. [[PubMed](#)]
8. Potter R, Haie-Meder C, Van Limbergen E, et al. Recommendations from gynaecological (GYN) GEC ESTRO working group (II): concepts and terms in 3D image-based treatment planning in cervix cancer brachytherapy-3D dose volume parameters and aspects of 3D image-based anatomy, radiation physics, radiobiology. *Radiother Oncol.* 2006;78:67–77. [[PubMed](#)]
9. Akimoto T, Katoh H, Noda SE, et al. Acute genitourinary toxicity after high dose rate (HDR) brachytherapy

- combined with hypofractionated external-beam radiation therapy for localized prostate cancer: second analysis to determine the correlation between the urethral dose in HDR brachytherapy and the severity of acute genitourinary toxicity. *Int J Radiat Oncol Biol Phys.* 2005;63:472–8. [[PubMed](#)]
10. Chassagne D, Dutreix A, Ash D, et al. Bethesda, MD: International Commission on Radiation Units and Measurements; 1997. ICRU report no 58: dose and volume specification for reporting interstitial therapy.
  11. Nose T, Koizumi M, Yoshida K, et al. In vivo dosimetry of high-dose-rate interstitial brachytherapy in the pelvic region: use of a radiophotoluminescence glass dosimeter for measurement of 1004 points in 66 patients with pelvic malignancy. *Int J Radiat Oncol Biol Phys.* 2008;70:626–33. [[PubMed](#)]
  12. Kim RY, Shen S, Lin HY, et al. Effects of bladder distension on organs at risk in 3D image-based planning of intracavitary brachytherapy for cervical cancer. *Int J Radiat Oncol Biol Phys.* 2010;76:485–9. [[PubMed](#)]
  13. Cengiz M, Gurdalli S, Selek U, et al. Effect of bladder distension on dose distribution of intracavitary brachytherapy for cervical cancer: three-dimensional computed tomography plan evaluation. *Int J Radiat Oncol Biol Phys.* 2008;70:464–8. [[PubMed](#)]
  14. Kirisits C, Lang S, Dimopoulos J, et al. The Vienna applicator for combined intracavitary and interstitial brachytherapy of cervical cancer: design, application, treatment planning, and dosimetric results. *Int J Radiat Oncol Biol Phys.* 2006;65:624–30. [[PubMed](#)]
  15. Yoshida K, Yamazaki H, Takenaka T, et al. A dose-volume analysis of magnetic resonance imaging-aided high-dose-rate image-based interstitial brachytherapy for uterine cervical cancer. *Int J Radiat Oncol Biol Phys.* 2010;77:765–72. [[PubMed](#)]

---

Articles from *Journal of Radiation Research* are provided here courtesy of **Oxford University Press**




Springerplus. 2013; 2: 424.

PMCID: PMC3769541

Published online 2013 August 30. doi: [10.1186/2193-1801-2-424](https://doi.org/10.1186/2193-1801-2-424)

## Eleven secondary cancers after hematopoietic stem cell transplantation using a total body irradiation-based regimen in 370 consecutive pediatric and adult patients

Mami Omori, Hideomi Yamashita,  Akihito Shinohara, Mineo Kurokawa, Jyunko Takita, Mitsuteru Hiwatari, and Keiichi Nakagawa


Departments of Radiology, University of Tokyo Hospital, 7-3-1, Hongo, Bunkyo-ku, 113-8655 Tokyo, Japan

Hematology and Oncology, University of Tokyo Hospital, Tokyo, Japan

Pediatrics, Graduate School of Medicine, University of Tokyo Hospital, Tokyo, Japan

Mami Omori, Email: [mami\\_oomori@yahoo.co.jp](mailto:mami_oomori@yahoo.co.jp).

[Contributor Information.](#)

 Corresponding author.

Received June 27, 2013; Accepted August 27, 2013.

[Copyright](#) © Omori et al.; licensee Springer. 2013

This article is published under license to BioMed Central Ltd. This is an Open Access article distributed under the terms of the Creative Commons Attribution License (<http://creativecommons.org/licenses/by/2.0>), which permits unrestricted use, distribution, and reproduction in any medium, provided the original work is properly cited.

### Abstract

Go to:

About the bone marrow transplantation that high dose chemotherapy and total-body irradiation (TBI) are used for as conditioning regimen, a late toxicity may become the problem in the long-term survival patient. One of the toxicities which has been implied to be associated with TBI is secondary carcinogenesis. Between June 1995 and December 2010, 370 patients who were undergoing allogeneic hematopoietic stem cell transplantation using a TBI-based regimen at our department, were the subjects of this study. Eleven secondary cancers occurred in 10 patients. The median time from transplantation to diagnosis of a secondary cancer was 6.8 years. In this analysis, the cumulative incidence rate of secondary cancer at 5 and 10 years was 2.15% and 6.46%, respectively after TBI in our institution.

**Keywords:** Total body irradiation, Secondary cancer, Bone marrow transplantation

### Introduction

Go to:

The conditioning regimen before allogeneic hematopoietic stem cell transplantation is intended to eradicate tumor cells and to promote immunosuppression to prevent graft rejection. A combination of cyclophosphamide and total body irradiation (TBI) is the most widely used regimen in transplantation for leukemia.

Patients who receive bone marrow transplantation underlie an increased risk for secondary cancers because of several risk factors, including radiation, chemotherapy, and immune stimulation. Several studies (Schneider et al. 2007; Bhatia et al. 1996; Witherspoon et al. 1989; Deeg & Witherspoon 1993; Witherspoon et al. 1992; Deeg et al. 1984) described the risk factors and incidence of secondary malignancy after transplantation.

We here report our single-center experience regarding second malignancy in patients treated with TBI-based regimen. This paper focuses on the occurrence of second solid cancer.

### Materials and methods

Go to:

## Patients

Between June 1995 and December 2010, 370 patients who were undergoing allogeneic hematopoietic stem cell transplantation using a TBI-based regimen at our department, were the subjects of this study. Data were obtained from our bone marrow transplantation (BMT) database.

## Transplantation procedure

The first choice of the preparative regimen is cyclophosphamide (Endoxan) 60 mg/kg div day -3, -2 and full TBI 2 Gy x2/day day -6, -5, -4 for acute myeloblastic leukemia (AML), acute lymphoblastic leukemia (ALL), myelodysplastic syndrome (MDS), chronic myeloblastic leukemia (CML). Calcineurin inhibitor [Cyclosporine A (Sandimmun) 3 mg/kg/day, cdiv day-1~ or FK506 (Tacrolimus) 0.03 mg/kg/day, cdiv day-1~] plus Methotrexate (MTX) day 1, 3, 6, 11 were administered to prevent GVHD.

A purpose of use of the immunosuppressive drugs in pediatric stem cell transplant is to control GVHD not to become severe. About the duration of administration, we reduce and cancel the immunosuppressive drug when GVHD becomes the minor degree not to affect everyday life. The period until coming to become able to control is not fixed because there is individual difference. In other words, we continue using an immunosuppressive drug for years for the case that GVHD aggravates when dose reduction. The kind of the immunosuppressive drug uses cyclosporine in the case of transplant between blood relatives and tacrolimus in the case of between unrelated blood relatives interval like the transplant of the adult.

## Total body irradiation

Patients were treated in a mobile box made of 10 mm thick polymethyl methacrylate 600 mm wide by 2000 mm long by 400 mm high. The box is capable of moving up to 250 cm forward and backward on the rails with a constant speed. Beam intensity and moving velocity defined dose rate in TBI (Ban et al. 2001). Normally, beam opening of the linac is 400 cm × 10 cm. Leukemia patients were usually treated in the supine position for three fractions in the morning and in the prone position for three fractions in the evening. The center of the mobile box was selected to be a reference point to attain the prescribed dose. Beam intensity and moving velocity were determined based on the measurement of the doses in Mix-DP slab phantoms with an ionization chamber, but no corrections for patient body size were required due to the use of the mobile box. Dose rate was 150 MU/min in all cases. Most commonly, a pair of customized metal blocks was placed on the mobile box for lung shielding. The blocks were fabricated according to the lung shape, which was obtained by use of the X-ray film taken in the box. Lung shielding was performed in a fraction of TBI out of six fractions for three consecutive days in most cases.

## Statistical analysis

The probability of the incidence of secondary cancer was estimated using the Kaplan-Meier method.

## Patients

The patients were 236 males and 134 females. The median age at transplantation was 36 years old (range; 1–72). The median follow-up time for only survivors was 10.5 years (max; 16.4). A hundred thirteen patients (31%) received transplantation for acute AML, 117 patients (32%) for ALL, 39 patients (11%) for lymphoma, 34 patients (9%) for MDS, 41 patients (11%) for CML, and six patients (1.6%) for dyshematopoiesis. Two hundred forty patients (65%) survived at least 1 year after TBI.

The conditioning regimens included TBI with cyclophosphamide (CY) alone (72%), etoposide (VP-16) alone (10%), or a combination of CY and VP-16 (18%). For pediatric case, melphalan (L-PAM), antithymocyte globulin (ATG), thiotepea (TESPA), or fludarabine were administered for ten, one, one, and two patients, respectively. Graft-versus-host disease (GVHD) prophylaxis consisted in the majority of patients of cyclosporine-A associated to methotrexate, and FK506 associated to methotrexate in some patients.